

# Asynchronous and Non-Stationary Interference Cancellation in Multiuser Interference Channels

Xin Cai, Zhitao Huang, and Baoguo Li

**Abstract**—A single antenna interference cancellation (SAIC) scheme is proposed. The scheme is motivated by the challenging asynchronous and non-stationary interference cancellation problem in wireless communications. Suppose the existence of the single-user region (SUR) of the desired signal, we propose to first recognize the SUR via a novel detection scheme. The SUR detection scheme proposed consists of the pseudo-observation matrix construction and the information theoretic criterion-based source number estimation. A basis set for the desired signal is then learnt over the SUR, via dictionary learning techniques. In the final signal recovery stage, a novel constrained sparse coding (CSC) process is proposed. The CSC reforms the conventional sparse coding (SC) via incorporating signal-specific constraints. Unlike existing SAIC algorithms, the proposed scheme is completely independent of a prior knowledge on the interferences. Numerical results are provided to demonstrate the effectiveness of the above proposed schemes under varied interference intensities and environmental noise levels. The proposed scheme outperformed competing SAIC schemes by about 5dB signal-to-interference-plus-noise ratio (SINR) improvement. The proposed CSC scheme outperformed the conventional SC by about 9dB SINR improvement, besides the superior recovery fidelity of signal property.

**Index Terms**—Asynchronous interference cancellation, non-stationary interference cancellation, single antenna interference cancellation, interference channels, signal recovery.

## I. Introduction

IN multiuser communication systems, the transmitters, commonly sharing a medium, send their messages to corresponding receivers. Due to the broadcast nature of the wireless channel, the desired signal of each user would interfere with other transmitted signals. In existing works dealing with interferences, it is often assumed that the desired and interfering signals arrive at each receiver simultaneously. However, the impracticality of the above presumption has been pointed out, and the asynchronism inherently existing in many communication systems requires consideration. For instance, in ad hoc networks, each node can communicate directly with other nodes without a central base station. Asynchronous interference would then occur when signals from different users arrive at a given receiver with arbitrary timing misalignments [1].

Xin Cai, Zhitao Huang and Baoguo Li are with the State Key Laboratory of Complex Electromagnetic Environment Effects on Electronics and Information System, National University of Defense Technology, Changsha, 410073, P.R. China (e-mail: williamxman@163.com, huangzhitao@nudt.edu.cn, laglbg322@163.com). This research is supported by the Program for Innovative Research Groups of the Hunan Provincial Natural Science Foundation of China (No.2019JJ10004).

## A. Related Works

Based on the number of antennas involved, existing techniques intended for asynchronous interference cancellation can be divided into two categories. The first, named multiple antenna interference cancellation (MAIC), applies to systems with an antenna array at the transmit and/or receiving end. In [2], to null out the asynchronous interference, a receiving array with space-time equalizer was designed based on objective optimization. In [3], the desired signal was coded by the precoding matrix at the transmit end, enabling subsequent recovery. The other category applies to systems with single antenna nodes, i.e., single antenna interference cancellation (SAIC). In [4], [5], asynchronous interference alignment (IA) was implemented in interference/X channels. The key idea of IA was to design signals such that they remained distinct from the interferences at the desired receivers [6]. IA-based schemes were limited by their reliance on the full state information on the asynchronous delays; meanwhile, relative delays considered in [4], [5] were confined to be within a symbol interval. A less limited technique for SAIC implemented the joint detection. In [7], joint symbol detection and channel estimation for both the desired and interfering signals were iteratively carried out. Though applicable under arbitrary delays among asynchronous signals, the scheme required that the number and modulation patterns of the interfering signals to be known.

The asynchronous interference issue becomes even more challenging under non-stationary scenario. This occurs for instance, in ad hoc networks with bursty traffic, where nodes are ‘active’ by certain chance, resulting in blocks of interfering users overlapped in part with the desired user [8]. In this paper, non-stationarity implies the changing number and patterns of the current active interfering signals. Since asynchronous interference cancellation schemes aforementioned often assumed known/fixed number and patterns, they are in general, incapable of dealing with non-stationary interferences. Existing works intended for or applicable to the non-stationary interference cancellation can also be divided as MAIC and SAIC. The former includes the semi-blind algorithms relying on training sequences [9], [10], and the blind beamformer in [11]. The latter includes the frequency shift (FRESH) filter proposed in [12], that exploited the cyclostationarity of communication signals. Theoretically, FRESH filter can extract the desired signal from interferences of arbitrary

number and patterns. However, in its fundamental form, the reliance on the reference signal (generally a known sequence of the very desired signal) hindered its practicality. Aiming at this deficiency, a blind adaptive FRESH (BA-FRESH) filtering technique was proposed in [13], in which a secondary branch was added as a proper reference. BA-FRESH filter and its improved versions had been adopted in [14], [15] for SAIC. However, BA-FRESH-based schemes still required the exact a priori knowledge on the cyclic spectrum of the desired signal, besides the cyclic disjointness between the desired and interfering signals. On the other hand, compressive sensing was applied for SAIC in [16]. The scheme presumed a sparse representation of the desired signal over a known basis. Moreover, the time-frequency (TF) distributions of the desired and interfering signals were expected to be intrinsically distinct. In our recent work [17], a three-stage SAIC scheme had been proposed, which exploited the recurrent property of the digitally-modulated signals and recovers the desired signal via template matching.

## B. Main Contributions

Due to limitations in implementation issues, SAIC is generally more practical than MAIC. In this paper, we are concerned with the cancellation of asynchronous and non-stationary interferences in multiuser systems with single antenna nodes. An interference cancellation scheme is proposed, aiming at recovering the desired signal from multiple interfering signals. The multi-stage scheme consists of the single-user region (SUR) detection, the basis set learning and the signal recovery via constrained sparse coding (CSC). Assuming the existence of the SUR of the desired signal, the modified information theoretic criterion (ITC) -based source number estimation technique is adopted for the SUR detection. A basis set is then learnt over the SUR, through the dictionary learning (DL) process. Based on the learnt basis set, the part of the desired signal contaminated by the interfering signals is reconstructed via the CSC, in which signal-specific constraint items are introduced in the conventional sparse coding (SC) to better facilitate the interference cancellation task.

In general, main contributions of the paper include:

- 1) The proposed SAIC scheme outperforms competing SAIC methods in terms of the recovery quality of the desired signal. About 5dB signal-to-interference-plus-noise ratio (SINR) improvement is achieved.
- 2) The proposed CSC scheme outperforms the conventional SC by about 9dB SINR improvement, besides the superior recovery fidelity of signal property.
- 3) Unlike existing SAIC schemes that require the number/patterns of the interferences or the state information on the asynchronous delays, the proposed scheme is completely independent of a prior knowledge on the interferences.
- 4) A novel SUR detection scheme is proposed, which can recognize accurately the SUR under varied interference intensities and environmental noise levels.

The paper is organized as follows. In Section II, the system model of the asynchronous and non-stationary interference scenarios, as well as the schematic diagram of the proposed scheme are introduced. The multi-stage interference cancellation scheme is presented in Section III. In Section IV, the discussion over the influence of the imperfect SUR is provided. Section V demonstrates representative numerical results. Finally, conclusions are drawn with remarks in Section VI.

**Notations:** Matrices and sets are denoted by uppercase boldface symbols. Vectors are denoted by lowercase boldface symbols.  $(\cdot)^R$  and  $(\cdot)^I$  indicate the real and imaginary parts of a complex number or vector.  $(\cdot)^T$  and  $(\cdot)^\dagger$  indicate the transpose and conjugate transpose of a vector.  $E\{\cdot\}$  is the expectation operator.  $\text{cov}(\mathbf{A})$  indicates the covariance matrix of  $\mathbf{A}$ .  $\langle \cdot \rangle$  is the inner product operator.  $\sigma(\cdot)$  indicates the standard deviation of a variant.  $|\cdot|$  indicates the absolute value or modulus.  $\|\cdot\|_F$  and  $\|\cdot\|_0$  denote the Frobenius norm and the  $l_0$  norm.  $\mathbb{C}$ ,  $\mathbb{R}$  and  $\mathbb{N}$  stand for the domains of the complex numbers, the real numbers and the integers, respectively.

## II. System Model

### A. Received Signal Model with Asynchronous and Non-stationary Interferences

Interference channel (IC) models a multiuser communication system where each transmitter communicates to its intended receiver while generating interference to other receivers [18]. Here we consider a multiuser IC with  $I$  transmit-receive pairs (i.e., there are  $I$  principal links between corresponding terminals and  $I(I-1)$  interference links), where each node is equipped with a single antenna. The received signal at the receiver  $i$ ,  $i = 1, 2, \dots, I$ , is defined as

$$x_i(t) = c_{ii}s_i(t - \tau_{ii}) + \sum_{j=1, j \neq i}^I c_{ji}s_j(t - \tau_{ji}) + n_i(t) \quad (1)$$

where  $c_{ii}$  is the channel coefficient of the principal link,  $c_{ji}$  ( $j \in [1, I]$ ,  $j \neq i$ ) is the channel coefficient of the interference link between the transmitter  $j$  and the receiver  $i$ . The free-space path loss (FSPL) channel is considered, and the propagations of all signals are assumed independent. Moreover, since the transmission rate is generally much faster than the channel variation rate, we assume that the channel coefficients are quasi-static (block-wise constant). The quasi-static model has been adopted widely in existing works including [2], [4], [5], [9]–[11], [17].  $s_i$  is the desired signal from the transmitter  $i$ ,  $s_j$  ( $j \in [1, I]$ ,  $j \neq i$ ) is the interfering signal from the transmitter  $j$ .  $\tau_{ji}$  ( $j \in [1, I]$ ) denotes the delay from the transmitter  $j$  to the receiver  $i$ .  $\tau_{ji}$  depends on the geometrical distribution of different nodes.  $n_i(t) \sim \mathcal{N}(0, \delta^2)$  denotes the additive white Gaussian noise (AWGN) on the receiver  $i$ ,  $\delta^2$  indicates the power of noise. In practice, users turn active by certain chances [19], resulting in different active intervals. Specifically, suppose

that  $s_j(t - \tau_{ji})$  ( $j \in [1, I]$ ) has non-zero power between  $t \in (T_j, T'_j)$ . Signals considered here can be expressed as:

$$s_j(t) = \sum_{q_j} A_{q_j} g_j \left[ t - (q_j - 1)T_B^j \right] \exp(j2\pi f_c^j t), j \in [1, I] \quad (2)$$

where  $A_{q_j}$  is determined by the  $q_j$ th transmitted symbol and the modulation pattern.  $g_j(\cdot)$  is the shaping pulse,  $T_B^j$  and  $f_c^j$  indicate respectively the symbol interval and carrier frequency. 'j' is the imaginary unit.

In this paper, we assume that:

1) There exists region within the received signal where only the desired user is active, i.e., the SUR of the desired signal.

2) The active interval of the desired user is known to the receiver. An aligned analysis window can hence be set to extract the original received signal. Since the desired user is active throughout the window, this would effectively avoid the SUR of the interferences. The knowledge on the active interval can be obtained via a time synchronization process<sup>1</sup>. Meanwhile, in case the synchronization fails or is too complex, the analysis window can be directly set to cover the whole received signal and alternative measures can be taken to avoid the SUR of the interferences, as will be described later.

Fig. 1 illustrates the received signal with asynchronous and non-stationary interferences. In this paper, 'asynchronous' and 'non-stationary' imply respectively the misaligned time-of-arrivals (TOA) and the varying number/patterns of the current active interfering signals.

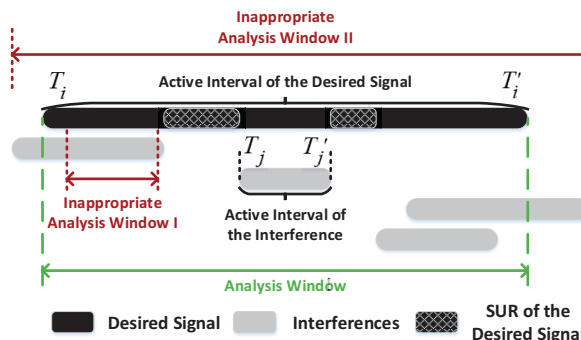


Fig. 1: The received signal with asynchronous and non-stationary interferences.

## B. System Overview

The framework of the proposed scheme is demonstrated in Fig. 2. The single channel received signal is first extracted by the analysis window and then expanded into the pseudo-observation matrix. The ITC-based source number estimation technique is then adopted for the SUR detection. Based on the detection results, the received signal is split into the SUR and the non-SUR. The former is loaded for the basis set learning, where the DL process is

<sup>1</sup>For details on time synchronization under the interferences, please refer to [20], [21] and references therein.

implemented. While the latter is prepared for the recovery of the contaminated desired signal, via the CSC. In the end, the SUR and the desired signal recovered from the non-SUR are integrated as the final recovered signal.

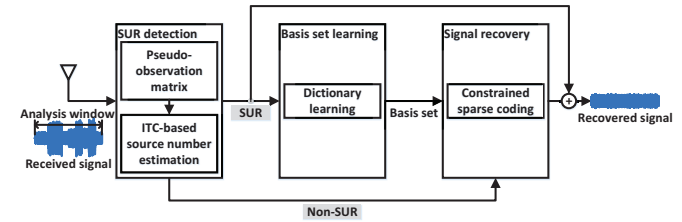


Fig. 2: Schematics of the proposed interference cancellation scheme.

## III. The Proposed Interference Cancellation Scheme

In this paper, we address the interference cancellation problem as recovering the desired signal from the received signal. The proposed scheme is inspired by the following observation: modulating is essentially mapping symbols from a finite alphabet onto corresponding waveforms. Communication signals are therefore the concatenation of recurrent temporal patterns. Consider the set  $\Phi$  consisted of short segments of one communication signal.  $\Phi$  can be split into two disjoint subsets  $\{\Phi_s, \complement_\Phi \Phi_s\}$  ( $\complement_\Phi \Phi_s$  indicates the complementary set of  $\Phi_s$ ). The recurrent property of communication signals implies that elements in  $\{\Phi_s, \complement_\Phi \Phi_s\}$  may actually lie in one common subspace spanned by a basis set  $\Omega$ . Based on the observation above, we propose to first split the received signal into the SUR and the non-SUR. Reasons for the division are: 1) Since in practice, the clean desired signal is generally unavailable as prior, the SUR may act as alternative training samples for the basis set learning; 2) Interference cancellation is only needed for the non-SUR; hence, this may avoid unnecessary computation load. The basis set  $\Omega$  is learnt over the SUR and the desired signal covered in the non-SUR is recovered by coding the non-SUR in the subspace spanned by  $\Omega$ .

### A. SUR Detection

As has been stated, we presume the existence of the SUR within the analysis window. For the division of the SUR and the non-SUR, certain SUR detection scheme is needed.  $x_i(t)$  in the analysis window is sampled and segmented into non-overlapping vectors  $\mathbf{x}_i^p \in \mathbb{C}^{1 \times L}$  ( $p \in [1, P]$ ,  $L$  is the segment length,  $P$  is the number of segments,  $P = N/L$ , where  $N$  is the total number of sample points). Suppose that the number of active users in  $\mathbf{x}_i^p$  is  $S^p$ , the SUR detection scheme aims at recognizing the subset  $\Phi_s$  of the vector set  $\Phi$  consisted of all  $\mathbf{x}_i^p$ , such that

$$\forall \mathbf{x}_i^p \in \Phi_s, S^p = 1 \quad (3)$$

The problem can be treated as a degraded source number estimation issue since we are only concerned with whether  $S^p = 1$ . Representative source number

estimation schemes include ITC-based ones, e.g., the minimum description length (MDL) algorithm [22], [23]. ITC-based algorithms avoid subjective threshold setting and implement the estimation via minimizing corresponding criteria. However, they require the observation dimension to exceed the latent source number [24], and hence cannot apply directly to the single antenna case. On the other hand, the concept of temporal linear array (TLA) was proposed in [25], as an intuitive way of constructing pseudo-observations in single antenna systems. Enlightened by the work in [25], we propose here a SUR detection scheme: for each  $\mathbf{x}_i^p$  ( $p \in [1, P]$ ), a pseudo-observation matrix  $\mathbf{X}_i^p$  is constructed via the TLA; ITC-based source number estimation method is then applied on  $\mathbf{X}_i^p$  to decide whether  $S^p = 1$ .

For  $\mathbf{x}_i^p$  ( $p \in [1, P]$ ), the construction of the pseudo-observation matrix  $\mathbf{X}_i^p$  is intuitive as in [25]

$$\mathbf{X}_i^p = [\mathbf{x}_i^{p,\mathbf{e}(1)}; \dots; \mathbf{x}_i^{p,\mathbf{e}(D)}] \quad (4)$$

where  $D$  is the pseudo-observation dimension,  $\mathbf{e} \in \mathbb{N}^{1 \times D}$  is the delay vector,  $\mathbf{e} = [0, 1, \dots, D - 1]$ . The  $d$ th ( $d \in [1, D]$ ) row of  $\mathbf{X}_i^p$ , i.e.,  $\mathbf{x}_i^{p,\mathbf{e}(d)}$  is formed as

$$\mathbf{x}_i^{p,\mathbf{e}(d)} = [\mathbf{x}_i^p(1+\mathbf{e}(d)), \mathbf{x}_i^p(2+\mathbf{e}(d)), \dots, \mathbf{x}_i^p(L-D+1+\mathbf{e}(d))] \quad (5)$$

Thus  $\mathbf{X}_i^p \in \mathbb{C}^{D \times (L-D+1)}$ . According to [25], the pseudo-observation matrix equals the observation matrix of an uniform linear array. In the proposed scheme,  $D$  is fixed at 3, as will be explained later. ITC-based schemes can then be applied on  $\mathbf{X}_i^p$  to determine whether  $S^p = 1$ . ITC-based source number estimation first formulates a family of conditional probability density functions  $y(\mathbf{X}|\mathbf{v}_k)$ , which depend on the assumed source number  $k$ .  $\mathbf{X}$  is the given observation matrix with dimension  $D$ ,  $\mathbf{v}_k$  is the parameter vector of the  $k$ th model ( $k \in [1, D - 1]$ ) [26]. ITC-based schemes aim at selecting the model that best fits the observation [22], [23]. Rissanen [23], [27] formulated the problem as selecting the model that yields the minimum description length of the observation, and the following MDL criterion is derived for the  $k$ th model:

$$\text{MDL}(k) = -\log y(\mathbf{X}|\hat{\mathbf{v}}_k) + \frac{1}{2}\omega \log C \quad (6)$$

in which  $\hat{\mathbf{v}}_k$  is the maximum likelihood estimation of  $\mathbf{v}_k$ ,  $\omega$  is the number of free parameters in  $\mathbf{v}_k$ ,  $C$  is the observation length of  $\mathbf{X}$ . The first term is the log likelihood function.

To actually apply the MDL criterion, the model requires first parameterization. According to [22], [26], the parameterization is based on the eigenstructure of the covariance matrix of  $\mathbf{X}$  (i.e.,  $\mathbf{R} = \text{cov}(\mathbf{X})$ ).  $\mathbf{R}$  can be expressed as

$$\mathbf{R} = \mathbf{\Xi} + \zeta^2 \mathbf{I} \quad (7)$$

where  $\mathbf{\Xi}$  denotes the covariance matrix of latent sources in  $\mathbf{X}$ ,  $\zeta^2$  indicates the noise power and  $\mathbf{I}$  is the identity matrix. The rank of  $\mathbf{\Xi}$  indicates the actual source number  $S$ , and can be determined by the multiplicity of the smallest eigenvalue of  $\mathbf{R}$  [26]. The problem can hence be formulated

as determining which of the family covariance matrices

$$\mathbf{R}_k = \mathbf{\Xi}_k + \zeta^2 \mathbf{I}, k \in [1, D - 1] \quad (8)$$

where  $\mathbf{\Xi}_k$  is a semi-positive matrix of rank  $k$  and  $\zeta^2$  is unknown, best fits the observation. With the well-known spectral representation theorem [22], [28],  $\mathbf{R}_k$  can be expressed as

$$\mathbf{R}_k = \sum_{j=1}^k (l_{k,j} - \zeta^2) \mathbf{u}_{k,j} \mathbf{u}_{k,j}^\top + \zeta^2 \mathbf{I} \quad (9)$$

where  $l_{k,j}$  and  $\mathbf{u}_{k,j}$  are respectively the eigenvalues and the eigenvectors of  $\mathbf{R}_k$ .  $\mathbf{v}_k$  is then

$$\mathbf{v}_k^\top = (l_{k,1}, \dots, l_{k,k}, \zeta^2, \mathbf{u}_{k,1}^\top, \dots, \mathbf{u}_{k,k}^\top) \quad (10)$$

Following [22], [29], the maximum likelihood estimations of elements in  $\mathbf{v}_k$  are

$$\begin{aligned} \hat{l}_{k,j} &= l_j, j = 1, \dots, k \\ \hat{\zeta}^2 &= \frac{1}{D - k} \sum_{j=k+1}^D l_j \\ \hat{\mathbf{u}}_{k,j} &= \mathbf{u}_j, j = 1, \dots, k \end{aligned} \quad (11)$$

where  $l_j$  and  $\mathbf{u}_j$  are respectively the  $j$ th eigenvalue and eigenvector of  $\mathbf{R}$ . The log-likelihood term in Eq. (6) for  $\mathbf{v}_k$  is then obtained as  $-(D - k)C \log \left( \frac{\prod_{j=k+1}^D l_j^{1/(D-k)}}{\frac{1}{D-k} \sum_{j=k+1}^D l_j} \right)$  [22], [26]. The number of free parameters in the  $k$ th model is counted as the degrees of freedom of the space spanned by  $\mathbf{v}_k$ , and hence  $\omega = k(2D - k) + 1$ .

After the above parameterization and maximum likelihood estimation of the parameters, the final form of MDL criterion is given for each  $k$  as (with  $k$ -irrelevant components removed)

$$\text{MDL}(k) = -(D - k)C \log \left( \frac{\prod_{j=k+1}^D l_j^{1/(D-k)}}{\frac{1}{D-k} \sum_{j=k+1}^D l_j} \right) + \frac{1}{2}k(2D - k) \log C \quad (12)$$

The estimated source number  $\hat{S}$  would be

$$\hat{S} = \arg \min_k \text{MDL}(k) \quad (13)$$

In the proposed scheme, we set  $D = 3$  and  $C = L - D + 1$ . According to Eq. (12), there would be

$$\text{MDL}(1) = \frac{5}{2} \log(L - 2) - 2(L - 2) \log \left[ \frac{(l_2 l_3)^{1/2}}{\frac{1}{2}(l_2 + l_3)} \right], \quad (14)$$

$$\text{MDL}(2) = 4 \log(L - 2)$$

in which  $l_j$  is the  $j$ th eigenvalue of the covariance matrix of  $\mathbf{X}_i^p$ . Based on [24] and our simulations, the eigenvalue structure of the covariance matrix is determined by  $S^p$ . For  $S^p = 1$  (SUR), the 1st eigenvalue ( $l_1$ ) would depend on the source power, while the last  $D - S^p$  eigenvalues ( $l_2, l_3$ ) all approximate the noise power under finite observation length. Under a moderate signal-to-noise ratio (SNR), there should be  $l_1 \gg l_2 \approx l_3$ . Hence, we have  $\text{MDL}(1) \approx \frac{5}{2} \log(L - 2) < \text{MDL}(2)$ , and the estimated source number  $\hat{S}^p = 1$ . For  $S^p > 1$  (non-SUR), it was

found in our simulations that  $l_1 \gg l_2 \gg l_3$ . Hence,  $\frac{l_2}{l_3} \gg 1$ , and  $\frac{(l_2 l_3)^{1/2}}{\frac{1}{2}(l_2 + l_3)} = \frac{(l_2/l_3)^{1/2}}{\frac{1}{2}(l_2/l_3 + 1)} \approx \frac{2(l_2/l_3)^{1/2}}{(l_2/l_3)} = 2(l_2/l_3)^{-1/2}$ . We have  $MDL(1) \approx \left[ (L-2) \log \left( \frac{l_2}{4l_3} \right) - \frac{3}{2} \log(L-2) \right] + 4 \log(L-2) > MDL(2)$ , and  $\hat{S}^p = 2$ . Fig. 3 illustrates the eigenvalues of the covariance matrixes corresponding to different  $S^p$ . Above analyses reveal the fact that, the proposed SUR detection scheme is capable of distinguishing between the SUR and the non-SUR. And  $\Phi$  can be divided into  $\Phi_s$  and  $C_\Phi \Phi_s$  based on  $\hat{S}_p (p \in [1, P])$ .

The possibility exists that  $\Phi_s = \emptyset$  after initial detections. This could occur when the SUR does exist but has been covered in hybrid segments (i.e., segments covering both the SUR and the non-SUR) under current sample rate and segment length. A resample may work as remedy in this case. Specifically, if  $\Phi_s = \emptyset$  after one round of reliable SUR detection<sup>2</sup>, the current sample rate could be raised by a ratio  $\varpi$  prior to a new round of detection.

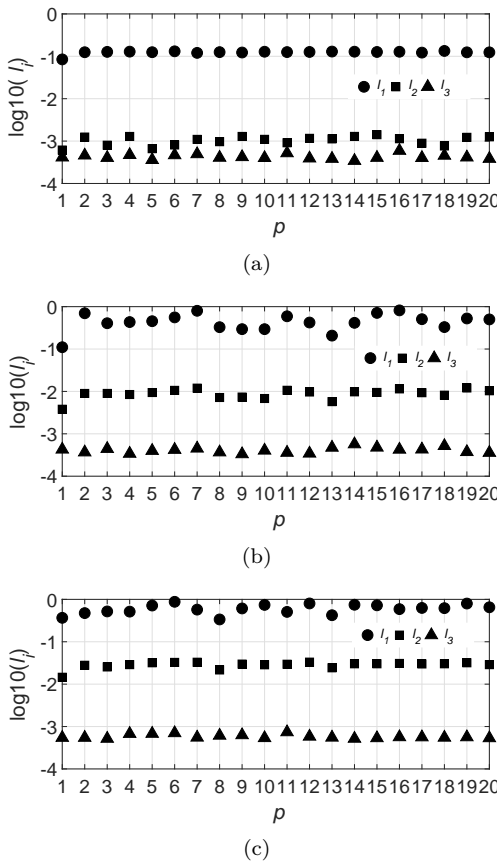


Fig. 3: Eigenvalues of the covariance matrixes corresponding to the SUR and the non-SUR. (a) SUR (b) Non-SUR ( $S_p = 2$ ) (c) Non-SUR ( $S_p = 3$ ).  $L = 500$ , SNR=20dB. Shown above are typical results of varied experiments implemented under different modulation patterns and  $L$ . Generally, we can see that in the SUR,  $l_1 \gg l_2 \approx l_3$ ; while in the non-SUR,  $l_1 \gg l_2 \gg l_3$ .

<sup>2</sup>Based on [24] and our experiments (see Tab. 2, Tab. 3),  $L$  could be selected within [500,1000] for reliable detection.

## B. Basis Set Learning

Elements in  $\Phi_s$  are essentially segmented desired signal with noise. Based on the recurrent nature of communication signals, we suppose the existence of a  $K$ -dimension subspace in which all elements of  $\Phi_s$  can be sparsely decomposed. Sparse decomposing of a vector relies highly on the degree of fitness between the data and the basis set. Among the state-of-the-art techniques for deriving data-driven bases, the DL schemes seek the dictionary leading to the best possible representations for each member in a training set. In the proposed scheme, the K-singular value decomposition (K-SVD) algorithm [30] is adopted to train the basis set  $\Omega$  over  $\Phi_s$ . K-SVD is an iterative method that alternates between sparsely decomposing the samples and updating the  $K$  candidate dictionary atoms (bases) by the singular value decomposition (SVD) computations. Under the sparsity-based mode, the scheme aims at solving the optimization problem below:

$$\min_{\Gamma, \Omega} \|\Psi - \Gamma \Omega\|_F^2 \text{ s.t. } \forall m \in [1, M], \|\Gamma_m\|_0 \leq U \quad (15)$$

in which  $\Psi \in \mathbb{R}^{M \times R}$  is the training sample set,  $M$  is the number of training samples,  $R$  is the dimension of one sample;  $\Gamma \in \mathbb{R}^{M \times K}$  is the sparse representation matrix,  $K$  is the total number of candidate bases;  $\Gamma_m$  is the  $m$ th row of  $\Gamma$ ;  $\Omega \in \mathbb{R}^{K \times R}$  is the basis set.  $U$  is the maximum number of non-zero elements allowed in  $\Gamma_m$ , i.e., the target sparsity.

The K-SVD algorithm consists of a sparse coding stage and a dictionary updating stage that iterate until convergence. In the sparse coding stage, certain pursuit algorithm is adopted to compute the representation vector  $\Gamma_m$  for each training sample  $\Psi_m$  ( $\Psi_m$  is the  $m$ th row of  $\Psi$ ), by approximating the solution of

$$\min_{\Gamma_m} \|\Psi_m - \Gamma_m \Omega\|_F^2 \text{ s.t. } \forall m \in [1, M], \|\Gamma_m\|_0 \leq U \quad (16)$$

In the dictionary updating stage, the  $k$ th ( $k \in [1, K]$ ) basis is updated by first computing the corresponding global representation error matrix  $\mathbf{E}_k$  as

$$\mathbf{E}_k = \Psi - \sum_{j=1, j \neq k}^K \Gamma^j \Omega_j \quad (17)$$

where  $\Gamma^j$  is the  $j$ th column of  $\Gamma$ ,  $\Omega_j$  is the  $j$ th row of  $\Omega$ .  $\mathbf{E}_k$  stands for the reconstruction error when the  $k$ th basis is removed from the current basis set. Then the SVD is applied to  $\mathbf{E}_k$  to find alternative  $\Omega_k$  by approximating  $\mathbf{E}_k$  as the closest rank-1 matrix. The algorithm obtains the updated dictionary by a total of  $K$  SVD computations, each determining one basis, and hence K-SVD. The iteration ends until the predefined maximum number of iterations  $\eta$  is met.

In the basis set learning stage of the proposed scheme, the training sample set  $\Psi$  is constructed over  $\Phi_s$ . Elements in  $\Phi_s$  are first concatenated in the original order as in  $x_i(t)$  to form the vector  $\mathbf{x}_{i, \Phi_s}$ . To maximize the number of available training samples,  $\mathbf{x}_{i, \Phi_s}$  is then segmented by a sliding window of length  $R/2$  into  $\{\mathbf{x}_{i, \Phi_s}^m | m \in [1, M]\}$ , with

overlap being  $(R/2) - 1$ .<sup>3</sup> The  $m$ th ( $m \in [1, M]$ ) training sample  $\Psi_m \in \mathbb{R}^{1 \times R}$  can be formed as  $[\left(\mathbf{x}_{i,\Phi_s}^m\right)^T, \left(\mathbf{x}_{i,\Phi_s}^m\right)^T]$ . In the proposed scheme,  $\Omega$  is initialized by selecting randomly  $K$  elements from the training sample set.

### C. Signal Recovery via the CSC

Presuming  $\Phi_s$  can be sparsely encoded in the  $K$ -dimension subspace spanned by  $\Omega$ , we attempt to recover the counterpart of the desired signal in  $\mathcal{C}_{\Phi}\Phi_s$  via coding  $\mathbf{x}_i^p \in \mathcal{C}_{\Phi}\Phi_s$  over  $\Omega$ . The signal recovery problem can be formulated as representing the given observation over a fixed basis set, under the sparsity constraint. The problem may be well solved by the SC technique, which aims at finding the sparsest representation that ‘best’ approximates a given observation. In this paper, the matching pursuit (MP) algorithm [31] is adopted and meanwhile tailored to better serve the interference cancellation task.

The basic idea of MP is to represent a vector  $\mathbf{x}$  as a weighted sum of bases using

$$\mathbf{x} = \sum_{l=1}^f \alpha_l \Omega_l^* + \mathbf{r}^f \quad (18)$$

where  $\mathbf{r}^f$  is the residual after  $f$  iterations, and  $\Omega_l^*$  is the basis that has the largest inner product with residual  $\mathbf{r}^{l-1}$ . At state  $l$ , the scheme identifies the basis in  $\Omega$  that best correlates with the current residual, that is

$$\Omega_l^* = \arg \max_{\Omega_k} \langle \mathbf{r}^{l-1}, \Omega_k \rangle, k \in [1, K] \quad (19)$$

The contribution of the chosen basis is then subtracted as follow:

$$\mathbf{r}^l = \mathbf{r}^{l-1} - \alpha_l \Omega_l^* \quad (20)$$

where  $\alpha_l = \langle \mathbf{r}^{l-1}, \Omega_l^* \rangle$  is the correlation coefficient. The process is repeated until the original vector  $\mathbf{x}$  is fully decomposed, e.g., the predefined maximum iteration  $f_m$  or reconstruction error tolerance reached. In the proposed scheme, the former stopping criterion is chosen and we set  $f_m = U$ , i.e., the target sparsity during the basis set learning. The reasons for such setting include: First, as asynchronous and non-stationary interferences are considered, it may be non-trivial to preset a fixed reconstruction error tolerance. Second, since  $\Omega$  is learnt under the sparsity constraint that each training sample can be decomposed by no more than  $U$  bases, it is rational to believe that the desired signal covered in  $\mathcal{C}_{\Phi}\Phi_s$  can also be reconstructed over  $\Omega$  under the same sparsity level. Finally, the reconstructed vector will be expressed as  $\sum_{l=1}^{f_m} \alpha_l \Omega_l^*$ .

Apparently, the iterative basis selection is crucial for the SC-based reconstruction. In the conventional MP, only the inner products between the candidate bases and the

<sup>3</sup>Suppose the length of  $\mathbf{x}_{i,\Phi_s}$  to be  $\gamma N$ , the number of segments is then  $M = \gamma N - \frac{R}{2} + 1$ . To learn a reliable basis set, we have after deduction  $R < 2k_{\text{sym}} \left[ \log_O \left( \frac{\gamma N}{\rho k_{\text{sym}}} \right) - 1 \right]$ , where  $O$  and  $k_{\text{sym}}$  are respectively the modulation order and the symbol oversample rate of the desired signal,  $\rho \in [1, 10]$ .

current residual are considered. The deficiencies include: First, the fidelity of critical properties of the desired signal is ignored. While such properties could be essential for the signal to hold its nature and distinctiveness, especially for the modulated signals concerned here. For instance, the constant modulus (CM) property of the Gaussian-filtered minimum shift keying (GMSK) and phase-shift keying (PSK) signals; or the constancy of the phase derivative of the pulse amplitude modulation (PAM) signals. Second, it would be hard to achieve a sufficient cancellation of interferences. Though the basis set is trained over the SUR of the desired signal, the non-zero inner products between the interfering part and the bases would be virtually inevitable, under the finite vector length. This would disturb the selection, especially under strong interference intensities or when the interferences correlate with the desired signal. Hence, the selection should be further constrained by discriminating items to prefer the desired signal. Meanwhile, the extra items may help maintain the critical properties of the desired signal.

To better fulfill the interference cancellation task, a constrained sparse coding scheme is proposed. Unlike the conventional MP, the CSC scheme selects basis in the  $l$ th iteration via

$$\Omega_l^* = \arg \max_{\Omega_k} \langle \mathbf{r}^{l-1}, \Omega_k \rangle + \sum_j \lambda_j G_j \left( \hat{\mathbf{s}}_{\Omega_a^k}^k \right), k \in [1, K] \quad (21)$$

in which  $G_j(\cdot)$  is the constraint item measuring certain property of the desired signal,  $\lambda_j \geq 0$  is the trade-off coefficient.  $\Omega_a^k$  indicates the union of the set  $\Omega_a$  consisted of bases already selected in previous  $l-1$  iterations and the current basis  $\Omega_k$  under evaluation.  $\hat{\mathbf{s}}_{\Omega_a^k}^k$  is the reconstruction result based on  $\Omega_a^k$ . Similar to the conventional MP that iterates between Eqs. (19), (20), the CSC iterates between Eqs. (21), (20). In the basis selection step of the  $l$ th iteration, all candidate bases  $\{\Omega_k | k \in [1, K]\}$  are evaluated by the integrated target function consisted of the inner product item and the constraint items in Eq. (21). For each  $\Omega_k$ , the inner product item is calculated as  $\alpha_l^k = \langle \mathbf{r}^{l-1}, \Omega_k \rangle$ . The constraint items are calculated by first obtaining the temporary reconstructed vector as  $\hat{\mathbf{x}}_l^k = \sum_{l'=1}^{l-1} \alpha_{l'} \Omega_{l'}^* + \alpha_l^k \Omega_k$ , where  $\{\Omega_{l'}^* | l' \in [1, l-1]\}$  constitutes  $\Omega_a$ . For the evaluation of  $G_j(\cdot)$ ,  $\hat{\mathbf{x}}_l^k$  is transformed into the original domain of the desired signal (e.g., from  $\mathbb{R}$  to  $\mathbb{C}$ ) as  $\hat{\mathbf{s}}_{\Omega_a^k}^k$ .  $\Omega_l^*$  is chosen as the  $\Omega_k$  that maximizes the target  $\alpha_l^k + \sum_j \lambda_j G_j \left( \hat{\mathbf{s}}_{\Omega_a^k}^k \right)$ . The residual is then updated by Eq. (20) with  $\alpha_l = \langle \mathbf{r}^{l-1}, \Omega_l^* \rangle$ , and  $\Omega_a$  is updated as  $\{\Omega_{l'}^* | l' \in [1, l]\}$ . The CSC iterates till the predefined maximum iteration  $U$ , and the final reconstructed vector will be  $\sum_{l=1}^U \alpha_l \Omega_l^*$ . For the kick-off of the iteration,  $\mathbf{r}^0$  and  $\Omega_a$  are initialized respectively as  $\mathbf{x}$  and  $\emptyset$ .

The constraint item  $G_j(\cdot)$  ensures that the fidelity of certain property of the clean desired signal is considered during the reconstruction. Moreover, as the inner product item and the signal-specific constraint item are of different nature, they can work collaboratively to fully exploit the distinctions between the clean desired signal and the

interfered one. These together, may help improve the quality of the recovered signal, as will be demonstrated. Notice that while all  $\lambda_j = 0$ , Eq. (21) degenerates back to the conventional MP. The constraint item  $G_j(\cdot)$  mainly measures critical algebraic or statistical property of the desired signal, by computing the difference between the clean desired signal and the recovered signal in terms of the property concerned. Conditions below should be considered when selecting  $G_j(\cdot)$ : 1) The clean desired signal and the interfered signal are distinct with regard to the property measured. 2) The item is computable over short segments. For instance, while the desired signal is the GMSK/PSK,  $G_j(\cdot)$  can be designed as  $G_1(\mathbf{z}) = -\sigma(|\mathbf{z}|)$ , which measures the constancy of the modulus of one vector. While the desired signal is amplitude-modulated such as the PAM, item measuring certain phase-related constancy can be chosen, e.g.,  $G_2(\mathbf{z}) = -\sigma(\varphi(\mathbf{z}))$ , where  $\varphi(\mathbf{z})$  computes the first order phase derivative of  $\mathbf{z}$  (after taking the remainder of  $\pi$ ), and hence  $G_2(\cdot)$  measures the constancy of the phase derivative (CPD) of one vector. Fig. 4 (a) (b) demonstrate the CM and the CPD properties of the clean GMSK and PAM signals, respectively.

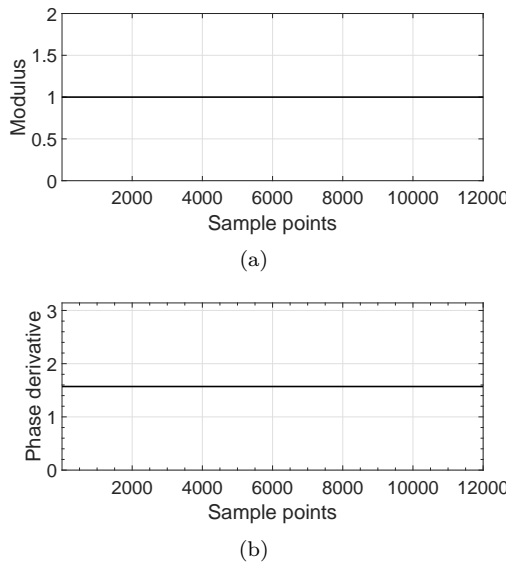


Fig. 4: Critical properties of the clean desired signals. (a) The CM property of the GMSK signal (b) The CPD property of the PAM signal.

In the signal recovery stage of the proposed scheme, to adopt the CSC for recovering the desired signal, the test sample set  $\Theta \in \mathbb{R}^{H \times R}$  ( $H$  is the number of test samples) is first constructed. Elements in  $\mathcal{C}_{\Phi}\Phi_s$  are concatenated in the original order as in  $x_i(t)$  to form the vector  $\mathbf{x}_{i,\mathcal{C}_{\Phi}\Phi_s}$ , which is then segmented in a non-overlapping manner by a window of length  $R/2$  into  $\{\mathbf{x}_{i,\mathcal{C}_{\Phi}\Phi_s}^h | h \in [1, H]\}$ <sup>4</sup>. The  $h$ th test sample  $\Theta_h \in \mathbb{R}^{1 \times R}$  is formed as  $\left[ \left( \mathbf{x}_{i,\mathcal{C}_{\Phi}\Phi_s}^h \right)^R, \left( \mathbf{x}_{i,\mathcal{C}_{\Phi}\Phi_s}^h \right)^I \right]$ . For each  $\Theta_h$ , the CSC

<sup>4</sup>Suppose the length of  $\mathbf{x}_{i,\mathcal{C}_{\Phi}\Phi_s}$  to be  $(1 - \gamma)N$ , the number of segments is then  $H = \frac{2(1-\gamma)N}{R}$ .

is applied to decompose it over  $\Omega$  via Eqs. (20), (21) under the target sparsity  $U$ .  $G_j(\cdot)$  is chosen according to the desired signal. After all  $\Theta_h$  have been reconstructed, the set of reconstructed vectors  $\{\hat{\mathbf{s}}_i^h | h \in [1, H]\}$  is synthesized, together with  $\{\mathbf{x}_i^p | \mathbf{x}_i^p \in \Phi_s, p \in [1, P]\}$  (rather than  $\{\mathbf{x}_{i,\Phi_s}^m | m \in [1, M]\}$ ), which are mutually overlapped), to form the final recovered desired signal  $\hat{\mathbf{s}}_i$ .

The proposed SAIC scheme for asynchronous and non-stationary interference cancellation is illustrated in Tab. 1.

Tab. 1: The proposed SAIC scheme for asynchronous and non-stationary interference cancellation

Input:	The received signal $x_i(t)$ , the segment lengths $L, R$ , the dimension of the basis set $K$ , the target sparsity $U$ .
Output:	The recovered desired signal $\hat{\mathbf{s}}_i$ .
1.SUR detection	
	Segment $x_i(t)$ in the analysis window into $\mathbf{x}_i^p \in \mathbb{C}^{1 \times L}$ ( $p \in [1, P]$ ) to form $\Phi$ .
	For $p = 1 : P$
	Construct $\mathbf{X}_i^p$ based on $\mathbf{x}_i^p$ via Eqs. (4), (5).
	Apply MDL on $\mathbf{X}_i^p$ to obtain $\hat{S}^p$ .
	End
	Construct $\Phi_s$ with $\{\mathbf{x}_i^p   \hat{S}^p = 1, p \in [1, P]\}$ .
2.Basis set learning	
	Construct the training sample set $\Psi \in \mathbb{R}^{M \times R}$ based on $\Phi_s$ .
	Initialize the basis set $\Omega \in \mathbb{R}^{K \times R}$ by selecting randomly $K$ samples from $\Psi$ , and the sparse representation matrix $\Gamma \in \mathbb{R}^{M \times K}$ by randomization.
	Do:
	For $m = 1 : M$
	Update the representation vector $\Gamma_m$ via Eq. (16), under the target sparsity $U$ , with $\Omega$ fixed.
	End
	For $k = 1 : K$
	Update the $k$ th basis via Eq. (17) and SVD, with $\Gamma$ fixed.
	End
	Until: Predefined iteration number.
3.Signal recovery	
	Concatenate and segment $\mathbf{x}_i^p \in \mathcal{C}_{\Phi}\Phi_s$ , $p \in [1, P]$ to form the test sample set $\Theta \in \mathbb{R}^{H \times R}$ .
	For $h = 1 : H$
	Apply the CSC on $\Theta_h$ via Eqs. (20), (21) over $\Omega$ under the maximum iteration $U$ .
	Obtain the recovered segment $\hat{\mathbf{s}}_i^h$ .
	End
	Synthesize $\hat{\mathbf{s}}_i^h$ ( $h \in [1, H]$ ) and $\Phi_s$ to form the final recovered desired signal $\hat{\mathbf{s}}_i$ .

#### IV. Discussions over the imperfect SUR

Assumptions 1), 2) in Section II imply the fact that: there should only exist the SUR of the desired signal. In this section, we provide basic discussions on how the proposed scheme would perform under its invalidity, i.e., the imperfect SUR. This could occur due to the inaccurate knowledge on the active interval of the current desired signal.

##### A. Non-existence of the SUR of the desired signal

The situation may occur due to inappropriate setting of the analysis window (as illustrated in Fig. 1, Inappro-

priate Analysis Window I) or the existence of continuous interferences. The recovery quality of the proposed scheme would be affected for the following reasons: 1) Since no or little SUR (due to possible false detection) would be recognized, there would be insufficient qualified training samples for the basis set learning. 2) The learnt basis set would be deformed and correlated with both the desired and interfering signals. The proposed scheme can then hardly distinguish the desired signal from the interferences. Solutions for the thorny situation could be adopting basis sets learnt elsewhere for the recovery of the desired signal in the current window.

### B. Existence of the heterogenous SUR

The heterogenous SUR indicates the situation where there exists the SUR not only of the desired, but also of the interfering signals. This occurs, for instance, when the interference arrives before the desired signal and is included in an inappropriate analysis window (as illustrated in Fig. 1, Inappropriate Analysis Window II). Without the loss of generality, suppose that there exists the SUR of the  $j^*$ th interference (denoted as  $\text{SUR}^{j^*}$ ), besides the desired signal. Influences of the heterogenous SUR, especially  $\text{SUR}^{j^*}$ , are two-folded: 1) The learnt basis set would be polluted. The bases are trained to not only sparsely represent segments of the desired signal, but also those of the  $j^*$ th interference. The learnt set is hence not discriminating enough to recover the desired signal from the  $j^*$ th interference. 2)  $\text{SUR}^{j^*}$  would not be included in  $\mathbb{C}_\Phi \Phi_s$  and would be loaded for signal recovery, and hence reserved in the recovered signal. This is less harmful since originally no desired part is included therein.

Luckily, damage of the polluted basis set is limited for the proposed scheme. This is because: 1) Among the multiple interferences, only the  $j^*$ th interference would be partly reserved (here we suppose a weak correlation between all signals). The basis set would still be capable of mitigating the energy of other interfering signals. 2) The signal-specific constraint item introduced would help distinguish between the desired signal-related and the interference-related bases. If the interference does not share the same characteristics of the desired signal, the scheme would tend to select the bases related to the latter, for the sake of better recovery fidelity.

Moreover, to avoid the existence of the heterogenous SUR, an intuitive post-checking module can be appended to the current SUR detection scheme. The signal-specific characteristics can be exploited again to verify whether the SUR recognized belongs to the desired signal. For instance, if the desired signal is known to be of constant modulus, the SUR with significant modulus fluctuations would be deemed as the interference and removed from both  $\Phi_s$  and  $\Phi$ .

## V. Numerical Results

Experiments have been conducted on an Intel(R) Core(TM) i7-6500U CPU @2.5GHz with Matlab R2016b

to demonstrate the performance of the proposed scheme under varied situations.

### A. Experiment 1

In this experiment, the proposed SUR detection scheme was tested. The received signal at the receiver #1 in a multiuser IC with  $I=5$  transmit-receive pairs was considered. Hence, the received signal consisted of the desired signal and four asynchronous interferences. The desired signal was QPSK, while the four interferences were respectively 4PAM, BPSK, 16-quadrature amplitude modulation (16QAM) and 4PAM. The number of sample points was  $N = 1.2 \times 10^6$ . In this experiment and others, the channel coefficients of all links were independently simulated and supposed to be quasi-static. To evaluate the detection performance, the false alarm rate (FAR) and the missing alarm rate (MAR) were adopted. The FAR indicated the proportion of the actual non-SUR segments falsely recognized as the SUR; the MAR indicated the proportion of the actual SUR segments falsely recognized as the non-SUR.

Tab. 2: The FAR of the proposed SUR detection scheme under varied SNR and  $L$ .

$\text{SNR}/\text{dB}$	100	250	500	750	1000
0	35.00%	18.33%	2.50%	1.25%	0.00%
5	27.67%	4.58%	0.00%	0.00%	0.00%
10	24.33%	2.92%	0.00%	0.00%	0.00%
15	22.00%	0.83%	0.00%	0.00%	0.00%
20	21.67%	0.00%	0.00%	0.00%	0.00%
25	21.17%	0.00%	0.00%	0.00%	0.00%
30	21.00%	0.00%	0.00%	0.00%	0.00%

Tab. 3: The MAR of the proposed SUR detection scheme under varied SNR and  $L$ .

$\text{SNR}/\text{dB}$	100	250	500	750	1000
0	1.00%	0.42%	0.00%	0.00%	0.00%
5	0.33%	0.00%	0.00%	0.00%	0.00%
10	0.00%	0.00%	0.00%	0.00%	0.00%
15	0.00%	0.00%	0.00%	0.00%	0.00%
20	0.00%	0.00%	0.00%	0.00%	0.00%
25	0.00%	0.00%	0.00%	0.00%	0.00%
30	0.00%	0.00%	0.00%	0.00%	0.00%

Tab. 2 and Tab. 3 list respectively the FAR and MAR under varied SNR and  $L$ . We can see from the tables that, the proposed SUR detection scheme was capable of accurately recognizing the SUR and the non-SUR segments, as both the FAR and the MAR reached 0% under moderate conditions. The SUR detection results are critical for the performance of the proposed interference cancellation scheme. Since it is based on the detection that  $\Phi$  is split into  $\Phi_s$  and  $\mathbb{C}_\Phi \Phi_s$ . Notice that the FAR rose under low SNR and small  $L$ . This was mainly because, the performance of the MDL scheme relied on the accuracy of eigenvalue computation [24], as can be seen from Eq. (12). While the eigenvalue computation was susceptible to the noise power and the dimensions of the pseudo-observation

matrix ( $D \times (L - D + 1)$ ). For the actual non-SUR segments,  $l_1 \gg l_2 \gg l_3$  and  $-2(L-2) \log \left[ \frac{(l_2 l_3)^{1/2}}{\frac{1}{2}(l_2+l_3)} \right] - \frac{3}{2} \log(L-2) > 0$ , hence  $\text{MDL}(1) > \text{MDL}(2)$ . However, the noise and limited observations would lead to errors (denoted as  $\varepsilon_j, j \in [1, 2, 3]$ ) in eigenvalues computed, and there would be  $\hat{l}_j = l_j + \varepsilon_j, j \in [1, 2, 3]$ . According to Eq. (14), there would be  $-2(L-2) \log \left[ \frac{(\hat{l}_2 \hat{l}_3)^{1/2}}{\frac{1}{2}(\hat{l}_2+\hat{l}_3)} \right] - \frac{3}{2} \log(L-2) < 0$ , i.e.,  $\text{MDL}(1) < \text{MDL}(2)$  while  $\left( \frac{\hat{l}_3}{\hat{l}_2} \right)^{-1/2} + \left( \frac{\hat{l}_3}{\hat{l}_2} \right)^{1/2} < 2(L-2)^{\frac{3}{4(L-2)}}$ . In that case, the actual non-SUR segment would be falsely recognized as the SUR, i.e., the false alarm. In both theory and our simulations, it was found that the stronger the noise and the shorter the observations, the larger the variance of  $\varepsilon_j$  and  $\frac{\hat{l}_3}{\hat{l}_2}$ . Since  $\left( \frac{\hat{l}_3}{\hat{l}_2} \right)^{-1/2} + \left( \frac{\hat{l}_3}{\hat{l}_2} \right)^{1/2}$  decreased as  $\frac{\hat{l}_3}{\hat{l}_2}$  rose, the probability that it dropped below  $2(L-2)^{\frac{3}{4(L-2)}}$  would be greater, i.e., higher FAR. A similar phenomenon was observed for the MAR, as it increased slightly under low SNR and small  $L$  as well. This could also be explained as above. Note that in terms of the performance of the proposed interference cancellation scheme, the FAR is more critical than the MAR. The rise of FAR would lower the quality of the recovered desired signal in that: First, the ‘fake SUR’ would be adopted as training samples in the basis set learning, and hence the learnt basis set may be polluted by the interfering signals covered in these segments. Second, since the signal recovery was applied only to  $\mathbf{x}_i^P \in \mathbb{C}_{\Phi}\Phi_s$ , such ‘fake SUR’ would be skipped without the interference cancellation. In contrast, the rise of MAR would only reduce to some extent the number of available training samples for the basis set learning. Though it can be seen from the tables that larger  $L$  was preferable to avoid high FAR and MAR, excessively large  $L$  would also be problematic as the larger  $L$  is, the wider regions covered in hybrid segments could be. The hybrid segments are intractable whether recognized as the SUR or the non-SUR. In this paper,  $L$  in [500, 1000] was suggested, based on our experiments.

## B. Experiment 2

In this experiment, the proposed interference cancellation scheme was tested. The desired signal was BPSK of the CM property and the interference was 4PAM<sup>5</sup>.  $(T_1, T'_1) = (0.01, 1)$ ,  $(T_2, T'_2) = (0.20, 1)$ .  $L=500$ ,  $R=80$ ,  $K=32$ ,  $U=3$ . The constraint item was  $G_1(\mathbf{z}) = -\sigma(|\mathbf{z}|)$  to measure the CM property of the clean BPSK signal.

Fig. 5 illustrates the quality of the recovered desired signal under varied SNR and  $\lambda_1$ , the signal-to-interference ratio (SIR) before recovery ( $\text{SIR}_B$ ) was -5.13dB. We can see from Fig. 5 (a) that the quality of the desired signal was remarkably promoted after the interference cancellation. The average SINR after recovery ( $\text{SINR}_A$ ) for  $\lambda_1 = 0, 30, 50, 100$  were respectively 3.07dB, 10.27dB, 12.11dB and

<sup>5</sup>Similar results had been obtained for extended interference modulations, e.g., BPSK, GMSK. These results are not shown due to limited space.

12.85dB. Comparing with the average SINR before recovery ( $\text{SINR}_B$ ), which was -5.32dB, promotions of 8.39dB, 15.59dB, 17.43dB and 18.17dB had been respectively achieved. This was also the case for the bit error rate (BER). For SNR=20dB, the BER before recovery ( $\text{BER}_B$ ) was  $1.61 \times 10^{-1}$ , while the BER after recovery ( $\text{BER}_A$ ) were respectively  $1.27 \times 10^{-1}$ ,  $5.63 \times 10^{-5}$ ,  $5.19 \times 10^{-5}$  and  $1.93 \times 10^{-4}$  for  $\lambda_1 = 0, 30, 50, 100$ . That is, the BER was reduced by up to 3 orders of magnitude. On the one hand, the recovery quality improved along with the SNR. This was mainly because: 1) The FAR and the MAR of the SUR detection rose as the SNR dropped. 2) The basis set  $\Omega$  was trained over  $\mathbf{x}_i^P \in \Phi_s$ , which was essentially contaminated by the environmental noise. These impaired the quality of the learnt basis set under strong noise. On the other hand, the superiority of the CSC over the conventional MP ( $\lambda_1=0$ ) was well illustrated. The average  $\text{SINR}_A$  for  $\lambda_1 = 30, 50, 100$  were respectively 7.20dB, 9.04dB and 9.78dB higher than that of the conventional MP. The phenomenon was even more pronounced in terms of the BER. Without the constraint item, the BER was scarcely improved. This was mainly because the inner product item alone was not discriminating enough to suppress the strong interference points by which error bits were originally induced. In the conventional MP, after the major part of the desired signal had been extracted in the early iterations, the interference component started to dominate the basis selection. The interference would eventually be reserved to a considerable extent, especially the strong interference points. Hence, the BER improvement would be quite limited, besides the insufficient SINR promotion. In contrast, the constraint item helped alleviate the disturbance of the strong interference on the basis selection. This was because the constraint item distinguished between the clean desired signal and the interfered one, by measuring the intrinsic property of the former. When the basis being evaluated introduced strong interference points in the recovered signal, it would be penalized by the constraint item and refrained from being selected.

Fig. 6 illustrates the quality of the recovered desired signal under varied  $\text{SIR}_B$  and  $\lambda_1$ , SNR=20dB. We can see that the  $\text{SINR}_A$  rose almost linearly along the  $\text{SIR}_B$ . This was mainly because, in our experiments, the interference was correlated with the desired signal (due to shared spectrum). Hence, the bases selected via Eq. (21) to reconstruct the desired signal would also correlate (though in a weaker sense) with the interference. And the energy of the interference reserved in the recovered signal would be proportional to the interference intensity. The CSC outperformed the conventional MP, under varied  $\text{SIR}_B$ . The average  $\text{SINR}_A$  for  $\lambda_1 = 30, 50, 100$  were respectively 6.84dB, 8.68dB and 9.07dB higher than that of the conventional MP. In terms of the BER, the  $\text{BER}_A$  dropped as  $\text{SIR}_B$  rose. Since as the interference became weaker, its disturbance on the basis selection process would be alleviated. Moreover, while the conventional MP failed to effectively reduce the BER, the CSC remarkably lowered the  $\text{BER}_A$ . For  $\text{SIR}_B=-5.13$ dB,  $\text{BER}_A$  under  $\lambda_1=0$  was

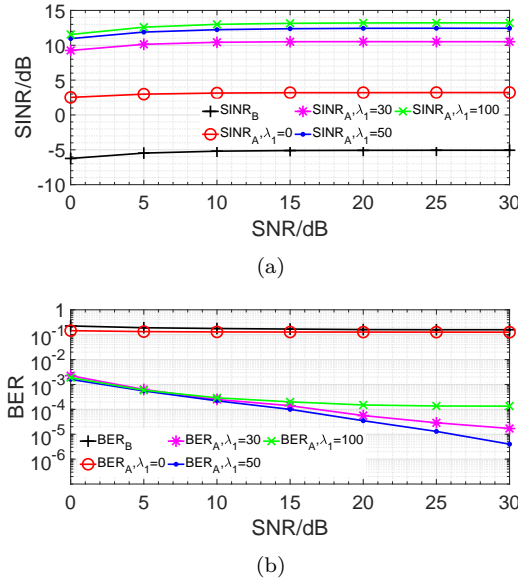


Fig. 5: The quality of the recovered desired signal under varied SNR and  $\lambda_1$ . (a) SINR (b) BER.  $\text{SINR}_B$  and  $\text{SINR}_A$  denote respectively the SINR before and after recovery.  $\text{BER}_B$  and  $\text{BER}_A$  denote respectively the BER before and after recovery.

$1.27 \times 10^{-1}$ . While the  $\text{BER}_A$  under  $\lambda_1=30, 50, 100$  were  $6.56 \times 10^{-5}, 5.19 \times 10^{-5}$  and  $2.10 \times 10^{-4}$  respectively. These can be explained as in the analyses of Fig. 5.

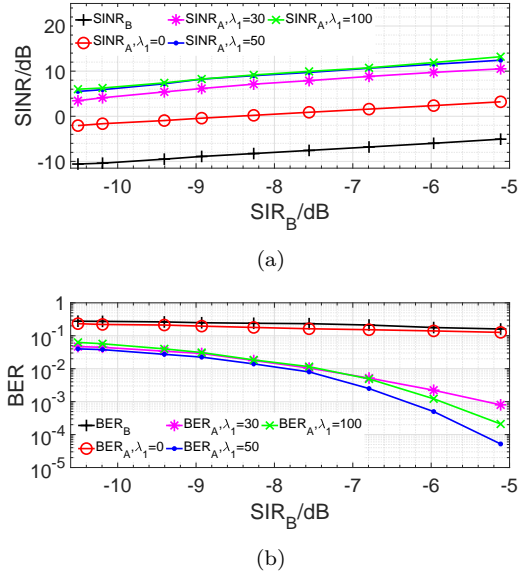


Fig. 6: The quality of the recovered desired signal under varied  $\text{SIR}_B$  and  $\lambda_1$ . (a) SINR (b) BER.

Fig. 7 demonstrates the desired signal, before and after the interference cancellation,  $\text{SIR}_B=-5.13$  dB,  $\text{SNR}=20$  dB. It can be seen that, the proposed scheme was capable of effectively mitigating the energy of the interference. The SUR was recognized and maintained in the recovered signal. On the one hand, comparison between Fig. 7 (c) and (d) reveals how the CM property of the desired signal was better reserved with the item  $G_1(\mathbf{z})$ . On the other

hand, we can see in Fig. 7 (c) that, the energy of the interference was notably reserved. As has been indicated, this should mainly be attributed to the disturbance on the basis selection by the strong interference here.

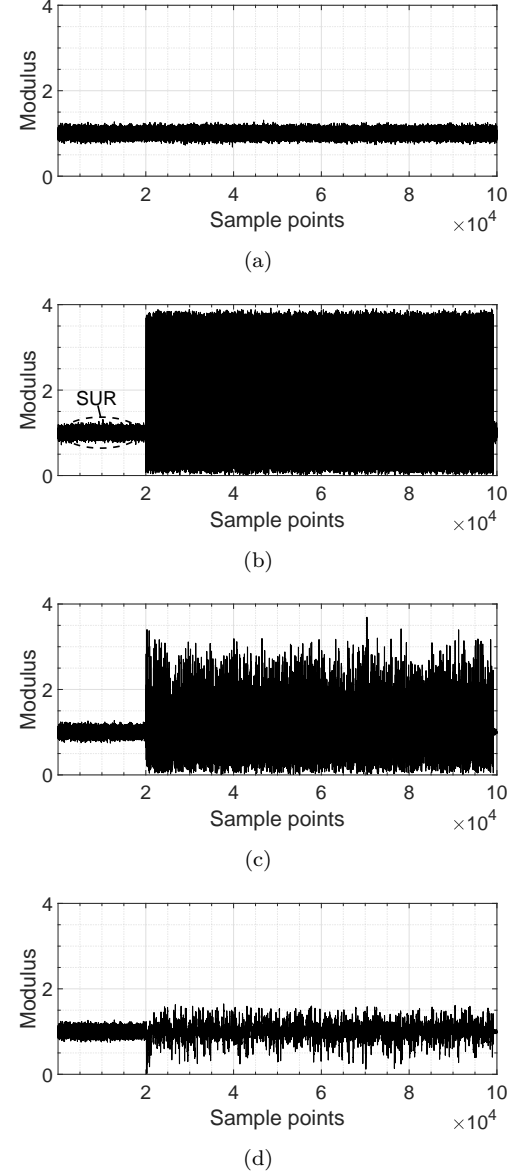


Fig. 7: The modulus of the desired signal before and after the interference cancellation. (a) The original desired signal with noise (b) The received signal including the desired signal and the interference (c) The recovered desired signal under  $\lambda_1=0$  (d) The recovered desired signal under  $\lambda_1=100$ .

### C. Experiment 3

In this experiment, the propose interference cancellation scheme was challenged by an intricate interference scenario. A multiuser IC with  $I=10$  transmit-receive pairs was considered. The desired signal was GMSK, which was interfered by 9 asynchronous interferences. The TOAs and active intervals of the interferences were randomly set, resulting in varied numbers of active interfering signals along

the transmission. Meanwhile, modulation patterns of the interferences covered the BPSK, QPSK, 2PAM, 4PAM, 16QAM and 32QAM. SNR=20dB, while the intensity of the global interference (when considering the multiple interferences as a whole) varied within the observation. In the proposed scheme, the system parameters remained the same as in Experiment 2. Fig. 8 demonstrates the spectrograms and the eye diagrams of the desired signal before and after the interference cancellation. We can see from the spectrograms that the energy of the asynchronous and non-stationary interferences had been effectively mitigated. The eye diagrams illustrated how the quality of the desired signal was promoted. Fig. 9 illustrates the real-time SINR of the desired signal along the transmission. The  $\text{SINR}_B$  and  $\text{SINR}_A$  were measured in a piecewise manner over an interval of 0.5s. We can see from the curves that in the non-SUR, at least 10dB promotion was achieved, under varied interference intensities.

#### D. Experiment 4

In this experiment, the proposed interference cancellation scheme was compared with existing SAIC schemes. Existing works in comparison included the scheme in [17] based on the SC and the template matching (SC-TM), the FRESH filter (FRESH) [12], the BA-FRESH filter (BA-FRESH) [15] and the conventional notch filter (NF). Tentative experiments had been carried out with the compressive sensing-based approach in [16]<sup>6</sup>. It was found that since the approach exploited the intrinsically different TF distributions to distinguish the desired signal from the interferences, it almost failed when all signals were digitally modulated with similar TF structures. The desired signal was BPSK with  $(T_1, T'_1)=(0.001, 1)$ . The two asynchronous interfering signals were BPSK with  $(T_2, T'_2)=(0.20, 0.60)$  and GMSK with  $(T_3, T'_3)=(0.50, 0.90)$ . In the proposed scheme,  $L=600$ ,  $R=72$ ,  $K=32$ ,  $U=3$ ,  $\lambda_1=1$ . For the SC-TM, since in its SUR detection stage, the residual tolerance required manual adjustment along with the SNR and SIR, we presumed that the true SUR was known (note that such a prior knowledge was only available for the SC-TM, not the proposed scheme). For the FRESH, the cycle frequencies adopted were  $\{-1/T_B^1, 0, 1/T_B^1\}$  and  $\{2f_c^1 - 1/T_B^1, 2f_c^1, 2f_c^1 + 1/T_B^1\}$ . The order of the linear-time-invariant (LTI) filter was  $L_f = 10$ . For the BA-FRESH, the received signal itself was loaded into the secondary branch as the reference. Perfect knowledge on the carrier frequencies and the bandwidths of the interferences was provided when constructing the notch filter.

Fig. 10 demonstrates the performance of the above schemes under varied  $\text{SIR}_B$ , measured by the  $\text{SINR}_A$ . SNR=20dB. It can be seen that the proposed scheme outperformed the SC-TM, the NF and the BA-FRESH, under varied interference intensities. The average  $\text{SINR}_A$  of the proposed scheme was 4.90dB, 5.33dB and 12.41dB

<sup>6</sup>Code of the approach is provided by the authors at <https://github.com/ElsevierSoftwareX/SOFTX-D-16-00102>.

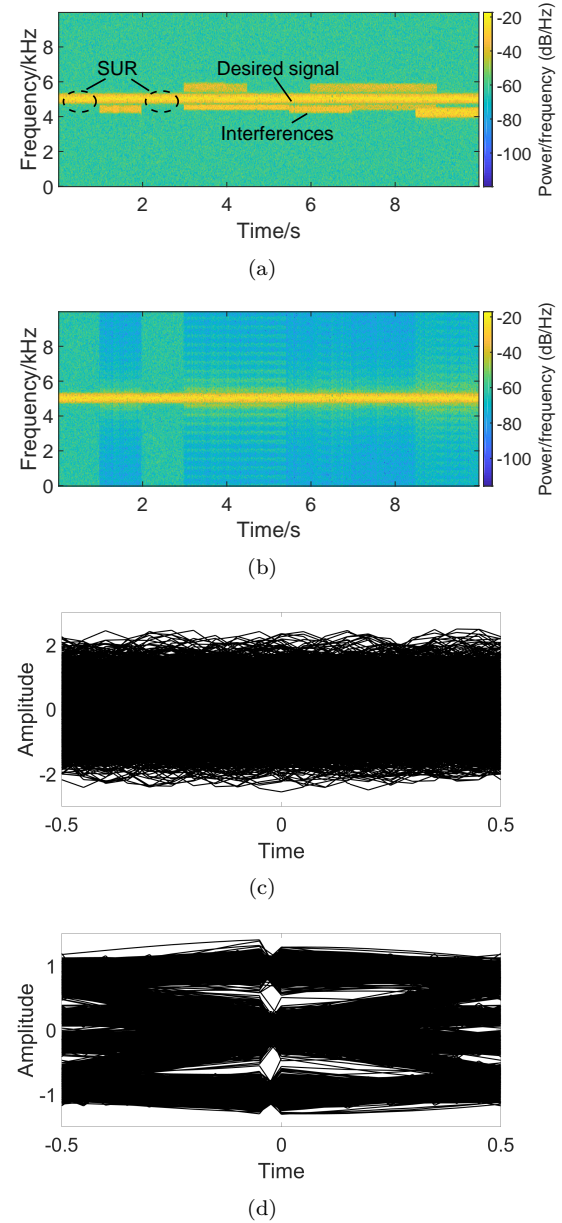


Fig. 8: The desired signal with asynchronous and non-stationary interferences before and after the interference cancellation. (a) The spectrogram before the interference cancellation (b) The spectrogram after the interference cancellation (c) The eye diagram before the interference cancellation (d) The eye diagram after the interference cancellation. The spectrograms were computed with a Hamming window of 256 points, 50% overlap between continuous sections and fast Fourier transform (FFT) of 256 points. The eye diagrams were drawn using the in-phase components of the signals. Each trace illustrated the input signal within one symbol duration. Note that the horizontal axis indicated time only in the normalized sense.

higher than that of the SC-TM, the NF and the BA-FRESH, respectively. The FRESH filter provided results better than those of the proposed scheme, with the exact desired signal as the reference and the perfect knowledge on the cyclic spectrum. The promotion over the SC-TM was remarkable, especially when it was given the true

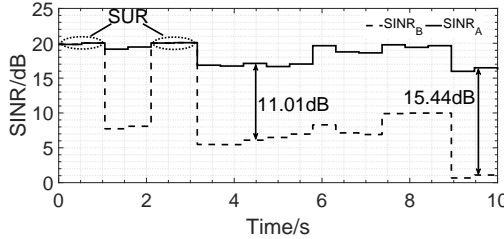


Fig. 9: The real-time SINR of the desired signal before and after the interference cancellation.

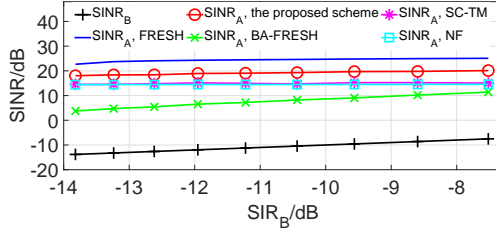


Fig. 10: The performance of the proposed scheme and existing SAIC schemes under varied  $SIR_B$ .

SUR while the proposed scheme was not. This indicated that first, the SUR detection scheme proposed here was more reliable; second, the signal recovery process in the proposed scheme outperformed the template matching in the SC-TM. Given perfect knowledge on the spectrum of the interferences, the NF provided results merely close to those of the SC-TM. This was because an ideal NF was impractical. The gap between the results of the FRESH and the BA-FRESH revealed the importance of a proper reference for the FRESH-based algorithms. When the desired signal was not available, their performance would degenerate even though the perfect knowledge on the cyclic spectrum was provided.

Fig. 11 demonstrates the performance of the above schemes under varied SNR,  $SIR_B = -13.50$  dB. We can see that the proposed scheme outperformed the SC-TM, the NF and the BA-FRESH, under moderate SNR. For SNR in [10,20] dB, the average  $SINR_A$  of the proposed scheme was 2.00dB, 4.77dB and 10.94dB higher than that of the NF, the SC-TM and the BA-FRESH, respectively. The SC-TM was inferior to the proposed scheme for SNR in [6,20] dB, and performed slightly better than the proposed scheme as the SNR dropped below 6dB. This was mainly because, the FAR of the proposed SUR detection scheme would rise under low SNR, and hence hindered the proposed scheme. In contrast, the SC-TM was given the true SUR. The NF and the BA-FRESH were rather insensitive to the environmental noise levels.

To further demonstrate the superiority of the CSC-based signal recovery over the template matching-based signal recovery [17], we provided a prior knowledge on the true SUR for both the proposed scheme and the SC-TM, and set the lengths of the individual bases in the two schemes to be identical. Fig. 12 illustrates the performance differences between the two schemes under varied  $SIR_B$  and SNR. It can be seen that the

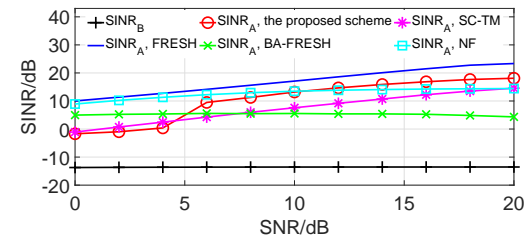


Fig. 11: The performance of the proposed scheme and existing SAIC schemes under varied SNR.

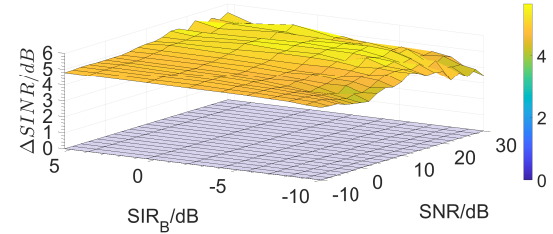


Fig. 12: The performance differences between the proposed scheme and the SC-TM under varied  $SIR_B$  and SNR. The performance difference was measured by  $\Delta SINR = SINR_{A, \text{Pro}} - SINR_{A, \text{SC-TM}}$ , where  $SINR_{A, \text{Pro}}$  and  $SINR_{A, \text{SC-TM}}$  indicate respectively the  $SINR_A$  of the proposed scheme and the SC-TM.

proposed scheme outperformed the SC-TM over the wide range of interference intensities and environmental noise levels. For  $SIR_B$  in [-10,5] dB and SNR in [-10,30] dB, the average  $\Delta SINR$  reached 4.83dB. This indicated that under moderate interference intensities, it was better to reconstruct the desired signal by the weighted sum of the bases, rather than simply one SUR segment. The iterative decomposing process in the CSC was more effective and reliable for reducing the reconstruction error. Moreover, since the true SUR was given in advance, the proposed scheme was no more hindered by the false alarm in its SUR detection stage.

In the end, we investigated the computation complexities of the proposed scheme and existing SAIC schemes. We supposed the total number of sample points to be  $N$  and the number of sample points covered in the SUR to be  $\gamma N$ . Meanwhile, let  $N_\alpha$  and  $L_n$  denote respectively the number of LTI filters in the FRESH/BA-FRESH and the notch filter order. Tab. 4 lists the approximate numbers of floating point operations (defined as the number of multiplications) in the above schemes. For the proposed scheme, each underlined item corresponds to one stage. In the SUR detection stage, the computations were mainly induced by obtaining the covariance matrix of  $\mathbf{X}_i^P$ . In the basis set learning stage, a total of  $\eta K$  SVD computations were implemented over  $\mathbf{E}_k \in \mathbb{R}^{M \times R}$ . It should be noticed that, for the dictionary updating, only the singular vector corresponding to the largest singular value was computed, rather than a complete SVD<sup>7</sup>. In the signal recovery stage,  $U$  CSC steps were respectively implemented over  $H$

<sup>7</sup>In Tab. 4, we presumed that the SVD was computed by the standard method in [32].

Tab. 4: Computation complexities of the proposed scheme and existing SAIC schemes.

The proposed scheme	$\frac{9N + \eta\gamma RK(U + K + 7R)N}{U(U + 6)K(1 - \gamma)N}, O(N)$
SC-TM	$\frac{4N^2 - 2NR}{R} + (1 - \gamma)\gamma\frac{4N^2}{R}, O(N^2)$
FRESH	$N_\alpha(2L_f + 1)N + 2N_\alpha^2 L_f N, O(N)$
BA-FRESH	$N_\alpha(2L_f + 1)N + 2N_\alpha^2 L_f N, O(N)$
NF	$L_n N, O(N)$

test samples. The constraint item was not computation-demanding as simple function was adopted. Notice that the split of the SUR and the non-SUR helped reduce the computational burden. The SC-TM required  $O(N^2)$  since in its SUR detection stage, each segment was coded by all other segments; meanwhile, in its signal recovery stage, each non-SUR segment was approximated by each SUR segment. The FRESH and the BA-FRESH were of close complexities, since the only difference lied in the reference signals adopted. Fig. 13 demonstrates the time consumptions of the above schemes under varied  $N$ .

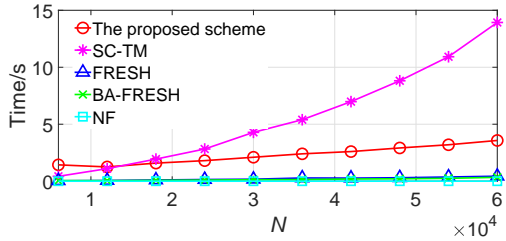


Fig. 13: Time consumptions of the proposed scheme and existing SAIC schemes.  $\eta = 10, \gamma = 0.1, L = 600, R = 72, K = 32, U = 3, N_\alpha = 6, L_f = 10, L_n = 10$ .

## E. Experiment 5

In this experiment, the proposed scheme was tested under the imperfect SUR, following the discussions in Section IV. We first tested the proposed scheme under the non-existence of the SUR, as discussed in Section IV. A. The signal parameters and algorithm settings remained unchanged as in Experiment 2, while the difference was that the interference overlapped with the desired signal throughout the analysis window. Besides testing the proposed scheme under varied SNR and  $SIR_B$ , we also evaluated the remedial solution proposed in Section IV. A that adopts the basis sets learnt elsewhere for the current recovery. Fig. 14 (a) illustrates the  $SINR_A$  under varied SNR and typical  $\lambda_1$ ,  $SIR_B = -6.11\text{dB}$ . The  $SINR_A$ -NonSUR indicates the recovery implemented via the routine procedures. Since no actual SUR existed in the current window, we had to train the basis set over the non-SUR. The  $SINR_A$ -SUR indicates the recovery implemented with the remedial solution. Specifically, under each SNR, the corresponding basis set learnt in Experiment 2 was applied directly. It can be seen from Fig. 14 (a) that, when the basis set was learnt over the non-SUR, the  $SINR$  promotion over the  $SINR_B$  was quite limited (the average

of  $SINR_A$ -NonSUR,  $\lambda_1 = 0$  was merely 0.65dB higher than that of the  $SINR_B$ ). This was because the basis set was essentially trained to reconstruct the linearly superimposed desired and interfering signals, hence the two parts were equally reserved during the recovery. The constraint item helped by selecting the bases preferring the desired signal (the average of  $SINR_A$ -NonSUR,  $\lambda_1 = 50$  was 2.78dB higher than that of the  $SINR_B$ ). However, since the bases themselves were deformed, the promotion remained limited. In contrast, the promotion in the  $SINR_A$ -SUR was remarkable. The average of  $SINR_A$ -SUR,  $\lambda_1 = 0$  and  $SINR_A$ -SUR,  $\lambda_1 = 50$  were respectively 8.22dB and 17.23dB higher than that of the  $SINR_B$ . Fig. 14 (b) illustrates the  $SINR_A$  under varied  $SIR_B$  and typical  $\lambda_1$ ,  $SNR = 20\text{dB}$ . Similar phenomena were observed in terms of how the performance of the proposed scheme deteriorated under the non-existence of the SUR and how the basis sets learnt elsewhere (for the desired signal of the same parameters) outperformed those learnt over the non-SUR. Above results and analyses reveal the meaningful fact that once a qualified basis set has been trained for a desired signal, it can be applied directly in different interference scenarios for the same desired signal. This avoids the repetitive basis training and may reduce significantly the time consumption.

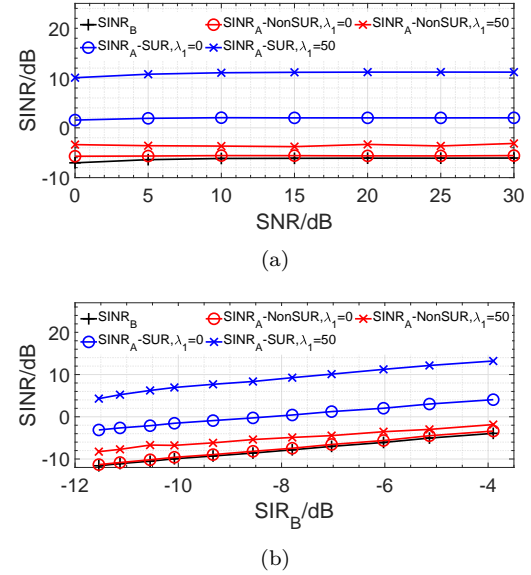


Fig. 14: The SINR after recovery under the non-existence of the SUR.

We also tested the proposed scheme under the existence of the heterogenous SUR, as discussed in Section IV. B. The desired signal was BPSK with  $(T_1, T'_1) = (0.001, 1.00)$ . The two interferences were 4PAM with  $(T_2, T'_2) = (0.80, 1.20)$  and GMSK with  $(T_3, T'_3) = (0.20, 0.90)$ . The analysis window was  $(0.001, 1.20)$ , hence there existed the SUR for both the desired signal and the interference No.1. The post-checking module proposed in Section IV. B was also evaluated. Fig. 15 (a) illustrates the  $SINR_A$  under varied

SINR and typical  $\lambda_1$ ,  $SIR_B = -0.25\text{dB}$ . The  $\text{SINR}_A$ -HeteSUR indicates the recovery implemented based on the original heterogenous SUR. The  $\text{SINR}_A$ -HeteSUR-PC indicates the recovery implemented with the post-checking. Specifically,  $\sigma(|\cdot|)$  was computed over each segment of the original SUR; the segments the corresponding values of which significantly exceeded the minimum of all were then discarded. We can see from Fig. 15 (a) that, based on the basis sets learnt over the heterogenous SUR, the average of  $\text{SINR}_A$ -HeteSUR,  $\lambda_1 = 0$  and  $\text{SINR}_A$ -HeteSUR,  $\lambda_1 = 50$  were only 1.16dB and 3.83dB higher than that of the  $\text{SINR}_B$ . This was mainly because the learnt bases can not effectively distinguish between the desired signal and the interference No.1, hence the latter was also reserved in the recovery. While with the post-checking, the recovery quality was remedied. The average of  $\text{SINR}_A$ -HeteSUR-PC,  $\lambda_1 = 0$  and  $\text{SINR}_A$ -HeteSUR-PC,  $\lambda_1 = 50$  were respectively 6.77dB and 9.51dB higher than that of the  $\text{SINR}_B$ . This should be attributed to the purified SUR. Through the post-checking, the SUR segments belonging to the interference No.1 were removed from  $\Phi_s$ . Hence, both interferences were effectively suppressed. The recovery results were explicitly shown as the spectrograms in Fig. 15 (b-d), where  $SIR_B = -0.25\text{dB}$ ,  $\text{SNR} = 20\text{dB}$ . It can be seen that, without the post-checking, only the interference No.2 was effectively removed; while with the post-checking, both interferences were remarkably suppressed. Notice that in the Fig. 15 (d), the SUR of the interference No.1 had been removed in the recovered signal.

## VI. Conclusions

The asynchronous and non-stationary interference cancellation problem is addressed. A multi-stage SAIC scheme is proposed, featuring the SUR detection, the basis set learning and the signal recovery. The SUR detection and the signal recovery stages are implemented respectively via the novel SUR detection scheme and the CSC process proposed. It is found that: 1) The proposed scheme can significantly improve the quality of the interfered desired signal, under varied  $SIR_B/\text{SNR}$ ; SINR promotion of over 15dB and BER improvement of 3 orders of magnitude are observed. 2) The proposed SAIC scheme outperforms competing SAIC schemes with better recovery quality (about 5dB SINR improvement is achieved). 3) The proposed CSC scheme outperforms the conventional SC in terms of the recovery quality measured by the SINR (about 9dB improvement is observed), the BER and the fidelity of critical characteristics. 4) The proposed SUR detection method provides satisfactory recognition rates, under varied SNR. We also discussed about the limited influence that the imperfect SUR may have on the performance of the proposed scheme. In general, the proposed scheme provides an effective meanwhile pragmatic solution for the asynchronous and non-stationary interference cancellation problem, as it applies to single antenna systems and requires literally no a prior knowledge on the interferences. Future work may focus on training the basis set

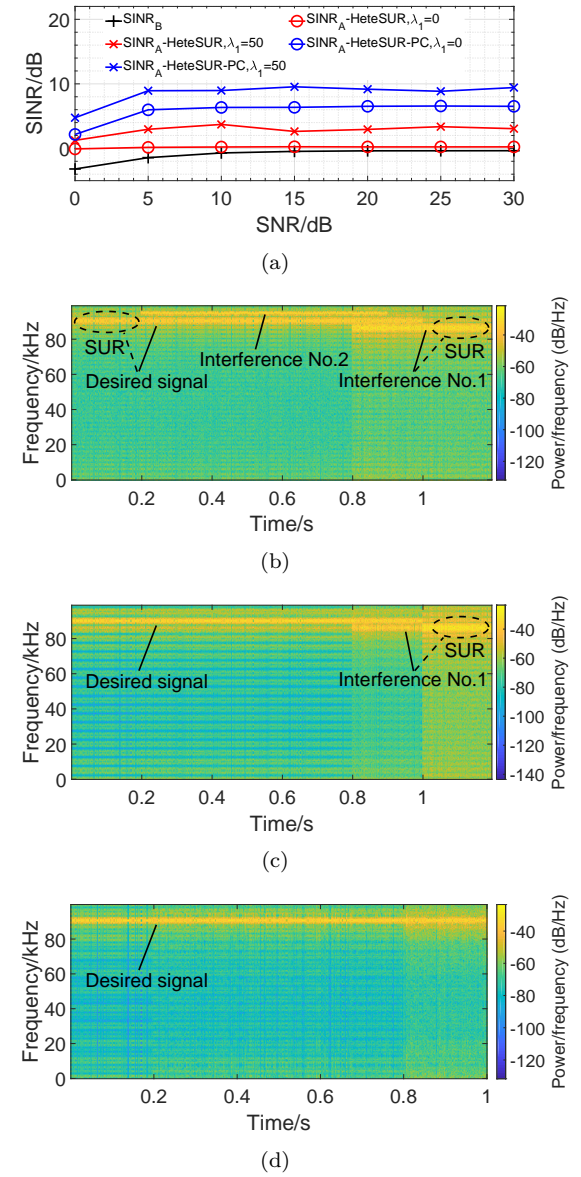


Fig. 15: The recovered desired signal under the existence of the heterogenous SUR. (a) The SINR after recovery (b) The spectrogram before recovery (c) The spectrogram after recovery without the post-checking (d) The spectrogram after recovery with the post-checking.

under strong environmental noise and extending to the application in multi-antenna systems.

## References

- [1] K. A. Hamdi, "Precise interference analysis of OFDMA time-asynchronous wireless ad-hoc networks," *IEEE Transactions on Wireless Communications*, vol. 9, pp. 134–144, Jan. 2010.
- [2] T. Tang and R. W. Heath, "A space-time receiver with joint synchronization and interference cancellation in asynchronous MIMO-OFDM systems," *IEEE Transactions on Vehicular Technology*, vol. 57, pp. 2991–3005, Feb. 2008.
- [3] S. B. Gee, Z. Lei, and Y. H. Chew, "Cooperative multiuser MIMO precoding design for asynchronous interference mitigation," in *IEEE GLOBECOM Workshops*, pp. 486–490, Mar. 2011.

- [4] H. Najafi, M. Torbatian, and M. O. Damen, "Interference alignment over asynchronous X networks," in IEEE International Symposium on Information Theory, pp. 2582–2586, Jul. 2011.
- [5] M. Torbatian, H. Najafi, and M. O. Damen, "Asynchronous interference alignment," IEEE Transactions on Wireless Communications, vol. 11, pp. 3148–3157, Jul. 2012.
- [6] M. A. Maddah-Ali, A. S. Motahari, and A. K. Khandani, "Communication over MIMO X channels: Interference alignment, decomposition, and performance analysis," IEEE Transactions on Information Theory, vol. 54, pp. 3457–3470, Jul. 2008.
- [7] Z. Zhou and T. Sato, "A blind single antenna interference cancellation algorithm for asynchronous OFDM communication systems," in IEEE 20th International Symposium on Personal, Indoor and Mobile Radio Communications, pp. 1226–1230, Apr. 2009.
- [8] B. Nosrat-Makouei, J. G. Andrews, and R. W. Heath, "User arrival in MIMO interference alignment networks," IEEE Transactions on Wireless Communications, vol. 11, pp. 842–851, Dec. 2011.
- [9] A. M. Kuzminskiy and Y. I. Abramovich, "Non-stationary multiple-antenna interference cancellation for unsynchronized OFDM systems with distributed training," Signal Processing, vol. 89, pp. 753–764, Oct. 2009.
- [10] F. A. Siddiqui, V. Srivastava, L. F. Danilo, and D. Falconer, "Suppression of intermittent interference using smart antenna with distributed training scheme," in Proceedings of 11th IEEE International Bhurban Conference on Applied Sciences & Technology, pp. 425–429, Mar. 2014.
- [11] M. Zhou and A. J. van der Veen, "Blind separation of partially overlapping data packets," Digital Signal Processing, vol. 68, pp. 154–166, Sept. 2017.
- [12] W. A. Gardner, "Cyclic Wiener filtering: theory and method," IEEE Transactions on Communications, vol. 41, pp. 151–163, Jan. 1993.
- [13] J. Zhang, K. M. Wong, Z. Luo, and P. Ching, "Blind adaptive FRESH filtering for signal extraction," IEEE Transactions on Signal Processing, vol. 47, pp. 1397–1402, May 1999.
- [14] L. Y. Ngan, S. Ouyang, and P. Ching, "Reduced-rank blind adaptive frequency-shift filtering for signal extraction," in IEEE International Conference on Acoustics, Speech and Signal Processing, pp. 650–653, Jun. 2004.
- [15] O. A. Y. Ojeda and J. Grajal, "Adaptive-FRESH filters for compensation of cycle-frequency errors," IEEE Transactions on Signal Processing, vol. 58, pp. 1–10, Jul. 2009.
- [16] L. Stanković, I. Orovčić, S. Stanković, and M. Amin, "Compressive sensing based separation of nonstationary and stationary signals overlapping in time-frequency," IEEE Transactions on Signal Processing, vol. 61, pp. 4562–4572, Jul. 2013.
- [17] Z. Huang and X. Cai, "Interference mitigation via sparse coding in K-user interference channels," IEEE Wireless Communications Letters, vol. 8, pp. 1596–1599, Dec. 2019.
- [18] L. Yang and W. Zhang, "On degrees of freedom region of three-user MIMO interference channels," IEEE Transactions on Signal Processing, vol. 63, pp. 590–603, Dec. 2014.
- [19] P. Cardieri, "Modeling interference in wireless ad hoc networks," IEEE Communications Surveys & Tutorials, vol. 12, pp. 551–572, May 2010.
- [20] J. Grotz, B. Ottersten, and J. Krause, "Joint channel synchronization under interference limited conditions," IEEE Transactions on Wireless Communications, vol. 6, pp. 3781–3789, Oct. 2007.
- [21] H. Kang, S. B. Im, H. J. Choi, and D. J. Rhee, "Robust OFDMA frame synchronization algorithm on inter-cell interference," in Asia-Pacific Conference on Communications, pp. 1209–1212, Aug. 2006.
- [22] M. Wax and T. Kailath, "Detection of signals by information theoretic criteria," IEEE Transactions on Acoustics, Speech and Signal Processing, vol. 33, pp. 387–392, Apr. 1985.
- [23] J. Rissanen, "Modeling by shortest data description," Automatica, vol. 14, pp. 465–471, Sept. 1978.
- [24] Q. T. Zhang, K. M. Wong, P. C. Yip, and J. P. Reilly, "Statistical analysis of the performance of information theoretic criteria in the detection of the number of signals in array processing," IEEE Transactions on Acoustics, Speech and Signal Processing, vol. 37, pp. 1557–1567, Oct. 1989.
- [25] X. Cai, X. Wang, Z. Huang, and F. Wang, "Single-channel blind source separation of communication signals using pseudo-MIMO observations," IEEE Communications Letters, vol. 22, pp. 1616–1619, May 2018.
- [26] K. M. Wong, Q. T. Zhang, J. P. Reilly, and P. C. Yip, "On information theoretic criteria for determining the number of signals in high resolution array processing," IEEE Transactions on Acoustics, Speech and Signal Processing, vol. 38, pp. 1959–1971, Nov. 1990.
- [27] J. Rissanen, "A universal prior for the integers and estimation by minimum description length," The Annals of Statistics, vol. 11, pp. 416–431, Nov. 1983.
- [28] S. Gilbert, Introduction to linear algebra. Wellesley, MA: Wellesley-Cambridge Press, 2016.
- [29] T. W. Anderson, "Asymptotic theory for principal component analysis," Annual of Mathematical Statistics, vol. 34, pp. 122–148, Oct. 1963.
- [30] M. Aharon, M. Elad, A. Bruckstein, et al., "K-SVD: an algorithm for designing overcomplete dictionaries for sparse representation," IEEE Transactions on Signal Processing, vol. 54, pp. 4311–4322, Oct. 2006.
- [31] S. G. Mallat and Z. Zhang, "Matching pursuits with time-frequency dictionaries," IEEE Transactions on Signal Processing, vol. 41, pp. 3397–3415, Dec. 1993.
- [32] G. H. Golub and C. Reinsch, "Singular value decomposition and least squares solutions," Numerische Math, vol. 14, pp. 403–420, Apr. 1970.

Xin Cai received his B.S. and M.S. degrees from the National University of Defense Technology, P. R. China. He is now pursuing his Ph.D. degree with the College of Electronic Science, National University of Defense Technology. His research interests include blind signal processing, machine learning et al.



Zhitao Huang received his B.S. and Ph.D. degrees from the National University of Defense Technology, P. R. China. He is now a professor of the National University of Defense Technology. His research interests include communication signal processing, array signal processing et al.



Baoguo Li received his B.S., M.S., and Ph.D. degrees from the National University of Defense Technology, P. R. China. He is now an associate professor of the National University of Defense Technology. His research interests include artificial intelligence in communication signal processing.

